THE JOURNAL OF BIOLOGICAL CHEMISTRY VOL. 292, NO. 8, pp. 3351–3365, February 24, 2017

Autoinhibition of the Nuclease ARTEMIS Is Mediated by a Physical Interaction between Its Catalytic and C-terminal Domains*[S]

Received for publication, November 30, 2016, and in revised form, January 12, 2017 Published, JBC Papers in Press, January 12, 2017, DOI 10.1074/jbc.M116.770461

Doris Niewolik[‡1], **Ingrid Peter**[§], **Carmen Butscher**[§], **and Klaus Schwarz**[‡§2]

From the [‡]*Institute for Transfusion Medicine, University of Ulm and the* [§]*Institute for Clinical Transfusion Medicine and Immunogenetics Ulm, German Red Cross Blood Service Baden-Wuerttemberg-Hessen, Ulm, Germany 89081*

Edited by Patrick Sung

The nuclease ARTEMIS is essential for the development of B and T lymphocytes. It is required for opening DNA hairpins generated during antigen receptor gene assembly from variable (V), diversity (D), and joining (J) subgenic elements (V(D)J recombination). As a member of the non-homologous end-joining pathway, it is also involved in repairing a subset of pathological DNA double strand breaks. Loss of ARTEMIS function therefore results in radiosensitive severe combined immunodeficiency (RS-SCID). The hairpin opening activity is dependent on the DNA-dependent protein kinase catalytic subunit (DNA-PKcs), which can bind to and phosphorylate ARTEMIS. The ARTEMIS C terminus is dispensable for cellular V(D)J recombination and *in vitro* nuclease assays with C-terminally truncated ARTEMIS showing DNA-PKcs-independent hairpin opening activity. Therefore, it has been postulated that ARTEMIS is regulated via autoinhibition by its C terminus. To obtain evidence for the autoinhibition model, we performed co-immunoprecipitation experiments with combinations of ARTEMIS mutants. We show that an N-terminal fragment comprising the catalytic domain can interact both with itself and with a C-terminal fragment. Amino acid exchanges N456A+S457A+E458Q in the C terminus of full-length ARTEMIS resulted in unmasking of the N terminus and in increased ARTEMIS activity in cellular V(D)J recombination assays. Mutations in ARTEMIS-deficient patients impaired the interaction with the C terminus and also affected protein stability. The interaction between the N- and C-terminal domains was not DNA-PKcs-dependent, and phosphomimetic mutations in the C-terminal domain did not result in unmasking of the catalytic domain. Our experiments provide strong evidence that a physical interaction between the C-terminal and catalytic domains mediates ARTEMIS autoinhibition.

The nuclease ARTEMIS is an essential factor of V(D)J[3] recombination, which is an obligatory step in the development of lymphocytes of the adaptive immune system (1, 2). During V(D)J recombination, the lymphocyte-specific recombination-activating gene products RAG1 and RAG2 cut sequence-specifically between the coding and signal sequences of the V-, D-, and J-gene segments, generating physiological DNA double strand breaks (DSB). At the coding joints, RAG1/2 generate hairpin structures, which subsequently are specifically opened by the nuclease ARTEMIS before religation can take place via the XRCC4-XLF-DNA ligase IV complex (3). Loss of ARTEMIS function results in the absence of B and T lymphocytes and in cellular hypersensitivity to ionizing radiation (IR). Patients diagnosed with this severe combined immunodeficiency with sensitivity to IR (RS-SCID) suffer from recurrent infections during infancy, and treatment by stem cell transplantation is necessary for survival. Thus, ARTEMIS is part of the non-homologous end-joining (NHEJ) pathway, which is important for the repair of naturally occurring and exogenously induced DNA DSB. ARTEMIS is composed of 692 amino acids (aa), and it can be divided into three distinct regions: the metallo-β-lactamase homology domain (aa 1–155); the β-CASP domain (aa 156–385, metallo-β-lactamase-associated CPSF ARTEMIS SNM1 PSO2), which together constitute the highly conserved catalytic domain; and the C-terminal region (aa 386–692) (4–6). The majority of ARTEMIS-deficient RS-SCID patients have gross deletions and missense or nonsense mutations in the catalytic domain (7). In addition to these null alleles, hypomorphic alleles have been described in patients with combined immunodeficiency (CID) of varying severity and in the radiosensitive Omenn syndrome (8–11). These mutations are associated with low numbers of polyclonal B and T lymphocytes, and they may predispose patients to lymphoma (8).

ARTEMIS associates with the DNA-dependent protein kinase catalytic subunit (DNA-PKcs) and acquires endonucleolytic activity on hairpins and DNA overhangs, as shown by *in*

* The authors declare that they have no conflicts of interest with the contents of this article.

[S] This article contains supplemental Tables S1 and S2.

[1] To whom correspondence should be addressed. Tel.: 49-731-150-6759; Fax: 49-731-150-645; E-mail: doris.niewolik@uni-ulm.de.

[2] Supported by Bundesministerium fuer Bildung und Forschung, Grant 01GM1517B.

[3] The abbreviations used are: V(D)J, variable (diversity) joining; aa, amino acid; ACTB, β-actin; ART-WT, full-length wild type ARTEMIS; ARM, ARTEMIS mutant; ATM, ataxia telangiectasia mutated; ATR, ataxia telangiectasia and Rad3-related; β-CASP, metallo-β-lactamase-associated CPSF ARTEMIS SNM1 PSO2; CID, combined immunodeficiency; Co-IP, co-immunoprecipitation; DNA-PKcs, DNA-dependent protein kinase, catalytic subunit; DSB, double strand break; ERK2, extracellular signal-regulated kinase 2; HPRT, hypoxanthine-guanine phosphoribosyltransferase; IMDM, Iscove's modified Dulbecco's medium; IP, immunoprecipitation; IR, ionizing radiation; NHEJ, non-homologous end-joining; N-N, self-interaction between the N-terminal domain of ARTEMIS; N-C, interaction between the N- and C-terminal domains of ARTEMIS; RS-SCID, combined severe immunodeficiency with radio-sensitivity; PTIP, Pax transactivation domain interaction protein.

vitro nuclease assays (2). In addition, ARTEMIS has an intrinsic DNA-PKcs independent exonucleolytic activity, which also resides in the N-terminal part of the protein (2, 12). In NHEJ-mediated general DNA repair, ARTEMIS is necessary for processing the DNA termini of a subset of DNA DSB induced by IR and other DNA-damaging agents (13). ARTEMIS is an *in vitro* substrate of the protein kinases DNA-PKcs, ataxia telangiectasia-mutated (ATM), and ataxia telangiectasia and Rad3-related (ATR), and the majority of phosphorylation sites are localized in the C-terminal tail of the protein (14–17). In response to DNA damage, ARTEMIS is hyperphosphorylated (13, 14, 16, 18–20). The DNA-PKcs binding region of ARTEMIS is located between amino acid positions 398 and 403 (17, 21). The exact role of the ARTEMIS C-terminal tail still is unclear, in particular in light of the fact that it is dispensable for V(D)J recombination and DNA repair (5, 21). Strikingly, a C-terminally truncated ARTEMIS mutant, which retains DNA-PKcs interaction, has DNA-PKcs independent activity on hairpins in the *in vitro* nuclease assay. This result is suggestive of the C-terminal region having a negative regulatory function, which may be relieved by DNA-PKcs-mediated phosphorylation (21). However, mutation of DNA-PKcs phosphorylation sites in the C-terminal tail of ARTEMIS has no effect on *in vivo* V(D)J recombination and DNA repair properties; rather autophosphorylation of DNA-PKcs was shown to regulate ARTEMIS endonucleolytic activities (16). Recently, DNA ligase IV (22–24) and the Pax transactivation domain interaction protein (PTIP) (25) have been shown to specifically interact with the C-terminal part of ARTEMIS.

NHEJ factors are in the focus as targets for cancer therapy, because of the reliance of tumor cell division on DNA repair mechanisms (26). Elucidation of the exact activation mechanisms of potential target proteins is a prerequisite for the development of novel therapeutic options. In the case of the nuclease ARTEMIS, advance has been impeded by the lack of any structural data of the full-length protein. Because of these limitations, we decided to employ classical biochemical methods to challenge the hypothesis of ARTEMIS being regulated by autoinhibition. Using co-immunoprecipitation experiments, we demonstrate that ARTEMIS interacts with itself in two ways, the N terminus can bind both to itself (N-N interaction) and to the C terminus (N-C interaction). In full-length ARTEMIS, specific amino acid exchanges within the C terminus impair the N-C interaction and confer an increase in V(D)J recombination activity. We show that missense mutations found in ARTEMIS-deficient patients affect the N-C, but not the N-N interaction and in addition influence protein stability. The presented data provide evidence that the formerly postulated ARTEMIS autoinhibition is mediated by a physical interaction between the catalytic and the C-terminal domains of the protein.

Results

ARTEMIS Can Self-interact—To test whether ARTEMIS is capable of self-interaction, we transiently co-expressed wild type ARTEMIS and different deletion mutants (Fig. 1*A*), containing at their C termini either a Myc or V5 tag. To avoid indirect co-immunoprecipitation, we performed the experiments in the CHO-derived cell line V-3, which is devoid of endogenous DNA-PKcs. Upon immunoprecipitation with anti-Myc antibody, eluates and input lysates were tested in Western blottings. These were sequentially probed with anti-V5 antibody to test for co-immunoprecipitation and anti-Myc antibody to detect the immunoprecipitate. Full-length ARTEMIS (ART-WT 1–692) was specifically co-immunoprecipitated by itself (Fig. 1*B*, *lanes 1–3*). The analyses of N- and C-terminal fragments showed that the N-terminal (ARM 1–382) but not the C-terminal part (ARM 414–692) of the ARTEMIS protein is capable of self-interaction (Fig. 1*B*, *lanes 5* and *14*, respectively). In addition, the non-overlapping N- and C-terminal fragments show reciprocal co-immunoprecipitations (Fig. 1*B*, *lanes 7* and *12*). To further characterize these two independent interactions, which we denote N-N and N-C interactions, we tested additional ARTEMIS deletion constructs. Deletion of amino acids 1–7 of the N-terminal fragment (ARM 8–382) retained co-immunoprecipitation of ARM 1–382 but resulted in loss of the interaction with ARM 414–692 (Fig. 1*B*, *lanes 6* and *13*, respectively). Deletion mutant ARM 474–692 shows reduced expression as compared with ARM 414–692. Therefore, in addition we performed a co-immunoprecipitation, in which cell lysate containing ARM 414–692 was diluted 1:4 with vector cell lysate (Fig. 1*B*, *lane 10*). Under these conditions, the amount of immunoprecipitated ARM 414–692 is comparable with that of mutant ARM 474–692, which appears as a doublet band. Whereas co-immunoprecipitation of the N-terminal fragment (ARM 1–382) is detectable for ARM 414–692, it is not for ARM 474–692 (Fig. 1*B*, compare *lanes 8* and *10*). Thus, amino acids between positions 414 and 474 in the C-terminal fragment are critical for the N-C interaction.

The extended C terminus of ARTEMIS contains several DNA-PKcs and ATM phosphorylation sites, and it was speculated to have a regulatory function. Therefore, we concentrated our further analyses on the characterization of the interaction between the N- and C-terminal ARTEMIS fragments. Because deletion of the first 7 amino acids at the N terminus is critical for the N-C interaction (Fig. 1*B*, compare *lanes 12* and *13*), we tested the effect of single amino acid exchanges in conserved positions within this region (see Fig. 1*C*). Expression levels of these mutant proteins are reduced compared with ARM 1–382, and this has to be taken into account in the interpretation of the results of the co-immunoprecipitation experiments. With the exception of amino acid exchange P12A, all mutations abolished co-immunoprecipitation by the C terminus (Fig. 1*D*). Thus, amino acid exchanges S2A, F4A, G6V, E10Q, and Y11A in the N-terminal fragment impair the N-C interaction. Next, we wanted to determine amino acids in the C-terminal fragment, which are crucial for binding to the N terminus. Analyses of additional deletion mutants revealed that binding is lost between amino acid positions 439 and 454 (data not shown). We therefore prepared C-terminal ARTEMIS mutants (aa 383–692) in which two or three adjacent amino acids were exchanged to alanine or in the case of acidic amino acids (Glu and Asp) to their corresponding amides (Gln and Asn). The expression levels of the different C-terminal proteins vary considerably (Fig. 1*E*, compare anti-V5 and anti-HPRT in *input*

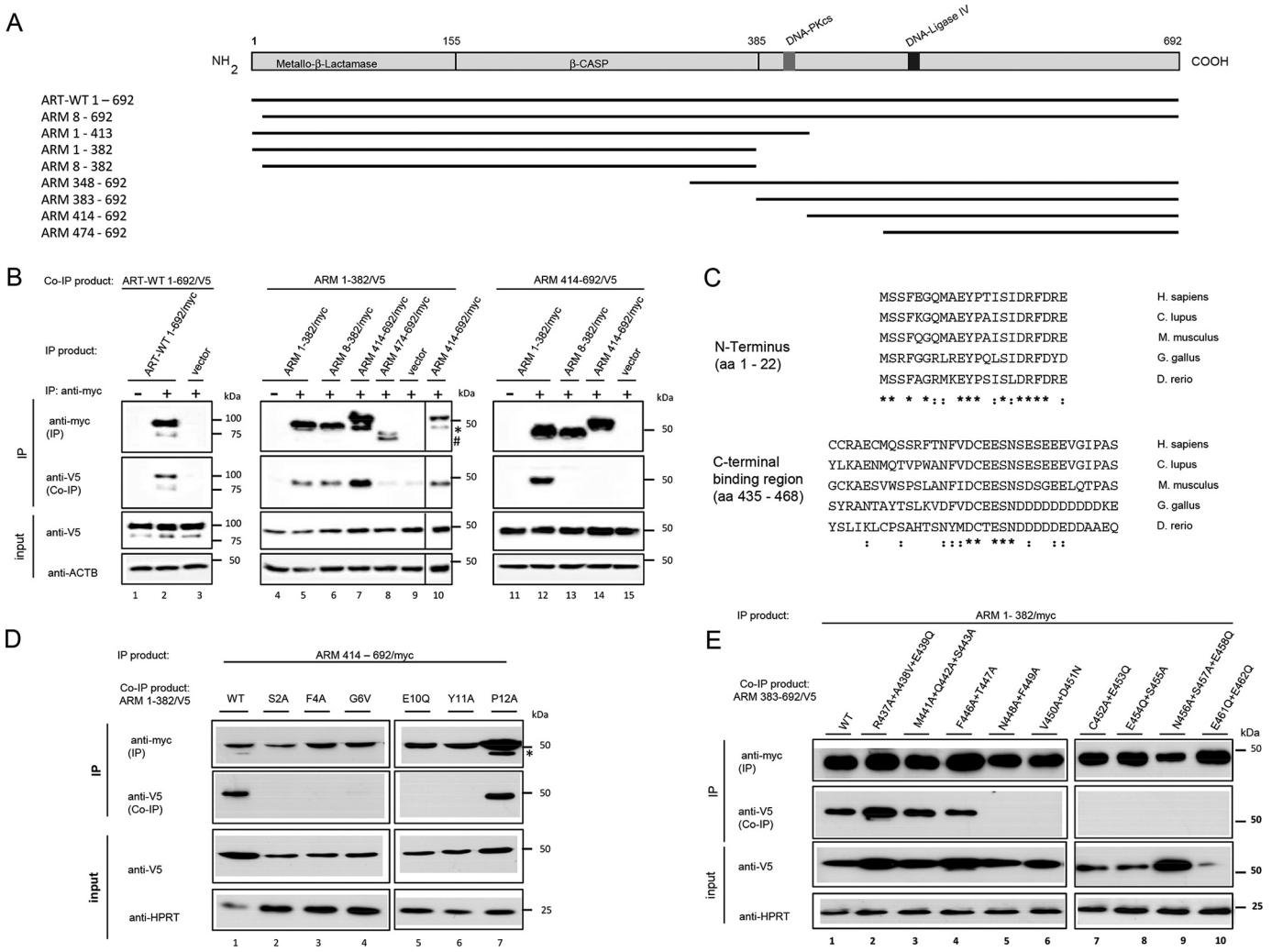

FIGURE 1. **ARTEMIS self-association, interaction between N- and C-terminal fragments is abolished by specific amino acid exchanges.** *A,* schematic presentation of ARTEMIS, indicating the metallo-β-lactamase and β-CASP domains and binding sites for DNA-PKcs and DNA ligase IV. *Numbers* at the top refer to amino acid positions. *Below*, N- and C-terminal deletion mutants (ARM) used in this study are represented as *black lines* and are specified at the *left* by name that defines the amino acids encompassed. *B*, *D,* and *E,* CHO V-3 cells were transfected with combinations of Myc- and V5-tagged wild type (*ART-WT*) or mutant (ARM) ARTEMIS-expressing plasmids or vector without insert. The Myc-tagged proteins were immunoprecipitated (*IP*) from cell lysates with anti-Myc antibody (+); IPs and input lysates were separated in SDS-PAGE, and Western blotting was performed. Co-immunoprecipitation (Co-IP) of the V5-tagged proteins was compared with input, using anti-V5 antibody. IP products were subsequently identified using anti-Myc antibody. *, band below 50 kDa in *B, lanes 7* and *10*, and in *D, lanes 1* and *7,* corresponds to the signal of the Co-IP, which was detected prior to the IP product. The position of protein standards is given at the *right* in kDa. Anti-β-actin (ACTB) and anti-HPRT antibodies were used as loading controls for *input lanes*. *B*, *lane 10*, co-immunoprecipitation was performed with a 1:4 mixture of lysates 7 and 9, respectively. #, ARM 474 – 692/myc (*lane 8*) is detectable as a doublet band. *C,* amino acids from the N- and C-terminal regions are compared between different species. *Asterisks* and *colons* indicate fully conserved and strongly similar residues, respectively (Clustal Omega). *D,* immunoprecipitation of the C-terminal fragment and co-immunoprecipitation of the N-terminal fragment with either wild type sequence or single amino acid exchanges as indicated at the top of the corresponding lanes. *E,* immunoprecipitation of the N-terminal fragment and co-immunoprecipitation of the C-terminal fragment with either wild type sequence or containing 2–3 amino acid exchanges as indicated at the *top* of the corresponding lanes. Transfection efficiencies were 88–99%. Each combination of expression plasmids was tested in at least three independent experiments. Representative experiments are shown. The binding activity of mutant P12A (*D, lane 7*) was somewhat variable: In three out of five experiments it was comparable with wild type. In one out of five experiments mutant E10Q (*D, lane 5*) also showed weak residual binding activity.

lanes). However, the capability to bind the N-terminal fragment (ARM 1–382) clearly is lost upon mutation of amino acids from positions 448 to 462 (Fig. 1*E*).

The experiments depicted in Fig. 1 define two non-overlapping regions of the ARTEMIS protein that bind to each other in co-immunoprecipitation experiments. Conserved amino acids at the very N terminus of ARTEMIS and in the C-terminal fragment are important for the N-C interaction. For simplicity, we refer to these separable protein binding regions hereafter as N- and C-terminal interaction domains. The N-terminal domain was also shown to have the capability to self-interact, and this interaction is not dependent on the 7 N-terminal residues (N-N interaction, Fig. 1*B*, *lanes 4–6*).

Single Point Mutations in the ARTEMIS N Terminus Also Affect V(D)J Recombination Activity—Previously, we have observed that deletion of the 7 N-terminal amino acids of full-length ARTEMIS (*ARM 8–692* in Fig. 1*A*) abolishes V(D)J recombination activity (9). To determine the functional effect of individual amino acid exchanges in the N-terminal fragment, we performed V(D)J recombination assays in ARTEMIS-deficient human primary skin fibroblasts. As controls, full-length ARTEMIS (ART-WT 1–692) as well as ARM 8–692 and ARM

8–382 were included in the analyses, and the expression levels of these proteins, in the absence of endogenous ARTEMIS, were analyzed in Western blottings (Fig. 2). The results of three independent cellular V(D)J recombination experiments are shown in Table 1. The recombination activity of C-terminally truncated ARTEMIS (ARM 1–382) is reduced 10–14-fold compared with ART-WT. However, because expression of ARM 1–382 is decreased about 100-fold as compared with ART-WT (Fig. 2, compare *lanes 1–4* with *lane 7*), its V(D)J recombination activity must exceed that of ART-WT. Deletion of the first 7 amino acids both in the full-length (ARM 8–692) and C-terminally truncated (ARM 8–382) proteins, results in reduction of V(D)J recombination activity to basal levels (−ART and −RAG1). In the case of ARM 8–692, this may in part be accounted for by the low expression levels as compared with ART-WT (Fig. 2, *lanes 1–5*). Yet, expression levels of ARM 1–382 and ARM 8–382 are comparable (Fig. 2, *lanes 7* and *8*, respectively), indicating that in the context of the C-terminally truncated proteins, the first 7 amino acids are important for V(D)J recombination activity. Each of the single point mutations tested abolished the V(D)J recombination activity of the C-terminally truncated ARM 1–382. This holds true also for mutation P12A, which showed binding activity toward the ARTEMIS C terminus in co-immunoprecipitation experiments (Fig. 1*D*, *lane 7*).

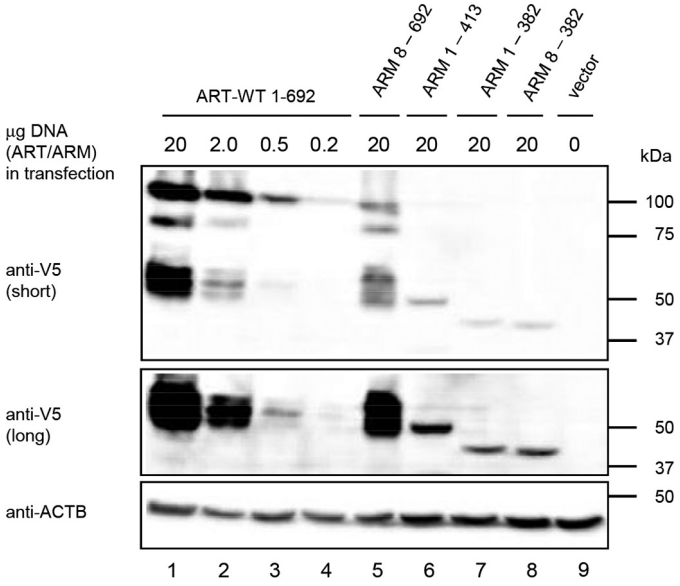

FIGURE 2. **Expression of wild type and truncated ARTEMIS proteins in ARTEMIS-deficient human primary skin fibroblasts.** ARTEMIS-deficient human primary skin fibroblasts were transfected with the indicated amounts of wild type (ART-WT) or mutant (ARM) ARTEMIS expression plasmids. Equal amounts of cell lysates were analyzed by SDS-PAGE and Western blotting. Anti-V5 antibody was used to detect ART-WT/ARM proteins, and anti-ACTB antibody was employed as loading control. A long exposure of the lower part of the gel is shown to detect the C-terminally truncated ARTEMIS proteins. The position of protein standards is given at the *right* in kDa. The experiment was performed three times with comparable results. Transfection efficiencies were 71–80%.

Full-length Wild Type ARTEMIS Cannot Interact with the Isolated C-terminal Fragment—The experiments shown in Fig. 1 were performed in the absence of endogenous DNA-PKcs to avoid indirect co-immunoprecipitation. Next, we wanted to establish whether full-length ARTEMIS also can interact with the N- and C-terminal fragments and, if so, whether binding of endogenous DNA-PKcs has an influence on these interactions. Hence, we carried out co-immunoprecipitation experiments in HEK293T cells. As expected, the mutations in ARM 1–692+L401G+R402N and deletion of the DNA-PKcs-binding site (ARM 1–382) abolish co-immunoprecipitation of endogenous DNA-PKcs (Fig. 3, compare *lanes 1–5* with *10–14* and *19–22*, respectively). ARTEMIS self-interaction is seen for both full-length proteins, as well as for the two N-terminal fragments ARM 1–413 and ARM 1–382, the latter of which does not contain the DNA-PKcs-binding site (Fig. 3, *lanes 1–4* and *10–13*). Surprisingly, the C-terminal fragment (ARM 414–692) is not co-immunoprecipitated by full-length ARTEMIS, irrespective of whether or not the precipitated ARTEMIS protein binds DNA-PKcs (Fig. 3, *lanes 5* and *14*). In HEK293T cells, specific interactions are observed both between the N-terminal fragments (Fig. 3, *lanes 19* and *20*) and the non-overlapping N- and C-terminal fragments (Fig. 3, *lanes 21* and *22*).

Although interaction with DNA-PKcs apparently is not the reason why the C-terminal fragment cannot bind to the N terminus in ART-WT, other protein-protein interactions could be responsible for masking the N terminus. Both intra- or intermolecular interactions between the N and C termini of full-length ARTEMIS or dimerization via the N-N interaction could theoretically be an explanation. To test this hypothesis, we analyzed the complete cassette of mutations that define the C-terminal interaction domain (see Fig. 1*D*) in full-length context (aa 1–692, wild type or mutant), asking whether any of the mutant proteins can interact with the isolated C-terminal fragment (ARM 414–692). This experiment was again performed in CHO V-3 cells, to avoid competition for binding with endogenous DNA-PKcs. In accordance with the results shown in Fig. 1, binding between the C- and N-terminal fragments is observed, and this interaction is lost if the first 7 amino acids at the N terminus are deleted (Fig. 4, *lanes 9* and *10*). Strikingly, two full-length mutant proteins show co-immunoprecipitation of

TABLE 1

V(D)J recombination assay in ARTEMIS-deficient human primary skin fibroblasts complemented with ARM containing deletions and single amino acid exchanges at the N terminus

Human primary skin fibroblasts were co-transfected with V(D)J recombination plasmid and plasmids expressing RAG1, RAG2, and one of the ARTEMIS proteins (wild type or mutant). As negative controls, the same co-transfections without the plasmids expressing RAG2 (−RAG2) or wild type ARTEMIS (−ART) were performed. In each assay 5×10^4 fibroblasts were analyzed by FACS analysis. The percentages of recombination-positive cells out of the subpopulation of transfected fibroblasts are shown.

	Controls						+ ARM 1–382 +					
	−RAG1	−ART	+ART-WT 1–692	+ARM 8–692	+ARM 1–382	+ARM 8–382	S2A	F4A	G6A	E10Q	Y11A	P12A
Exp. 1	0.05	0.05	2.88	0.03	0.26	0.01	0.06	0.01	0.01	0.05	0.08	0.02
Exp. 2	0.05	0.04	1.65	0.03	0.12	0.02	0.04	0.03	0.01	0.02	0.02	0.01
Exp. 3	0.05	0.06	1.85	0.03	0.17	0.04	0.03	0.04	0.03	0.05	0.05	0.04

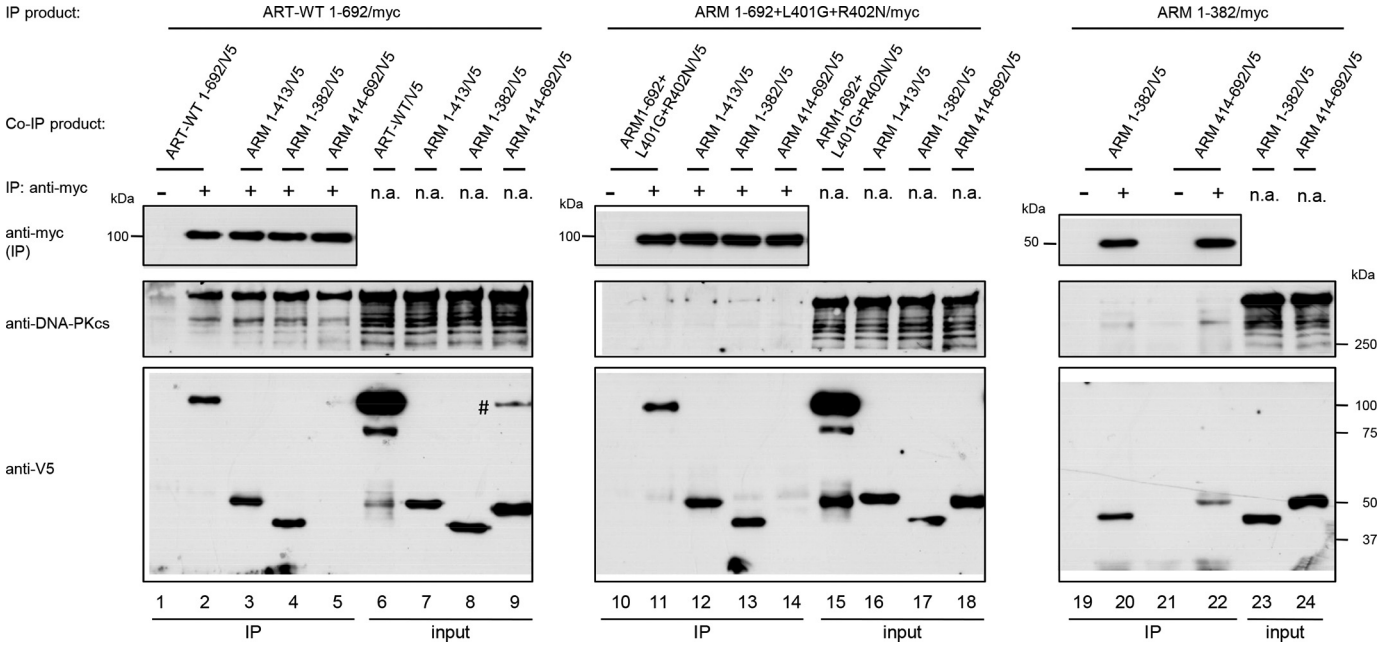

FIGURE 3. **Full-length ARTEMIS can interact with N-terminal but not with C-terminal ARTEMIS fragments.** HEK293T cells were transfected with combinations of Myc- and V5-tagged ARTEMIS expressing plasmids as indicated (see Fig. 1*A*). Protein interactions were subsequently analyzed by Co-IP, see legend to Fig. 1 for details. Membranes were probed with anti-DNA-PKcs, anti-V5, and anti-Myc antibodies to detect Co-IP and IP products. *n.a.* indicates not applicable. # indicates artifactual band. The experiment was performed twice with comparable results. The transfection efficiencies were 71–83%.

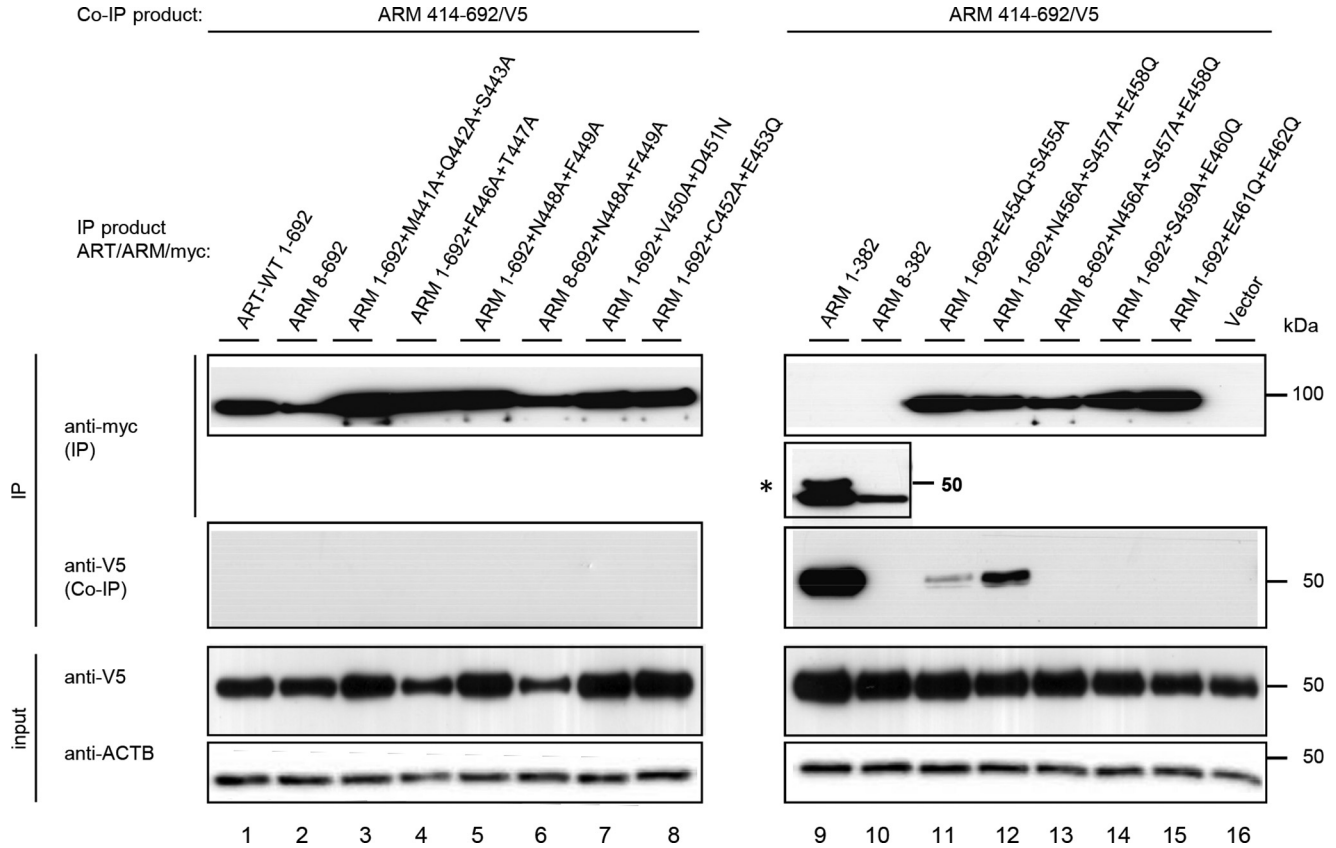

FIGURE 4. **Specific amino acid exchanges within the C-terminal interaction domain of full-length ARTEMIS induce co-immunoprecipitation of the isolated C-terminal fragment.** CHO V-3 cells were transfected with the V5-tagged C-terminal fragment (ARM 414–692) in combination with Myc-tagged full-length wild type (ART-WT) or mutant (ARM) ARTEMIS expressing plasmids as indicated. Each mutant is specified by the amino acids encompassed and the specific amino acid exchanges. Protein interactions were subsequently analyzed by Co-IP, see legend to Fig. 1 for details. Membranes were probed with anti-V5 and anti-Myc antibodies to detect Co-IP and IP products, respectively. Anti-ACTB antibody was used as loading control for *input lanes*. The experiment was performed twice, with a comparable outcome. Depicted is the result of the more sensitive experiment, showing also weak Co-IP by mutant ARM 1–692+E454Q+S455A, in addition to mutant ARM 1–692+N456A+S457A+N458E (*lanes 11* and *12*, respectively). *, band above 50 kDa in *lane 9* corresponds to the signal of the co-immunoprecipitate, which was detected prior to the IP product. Transfection efficiencies were 90–93%.

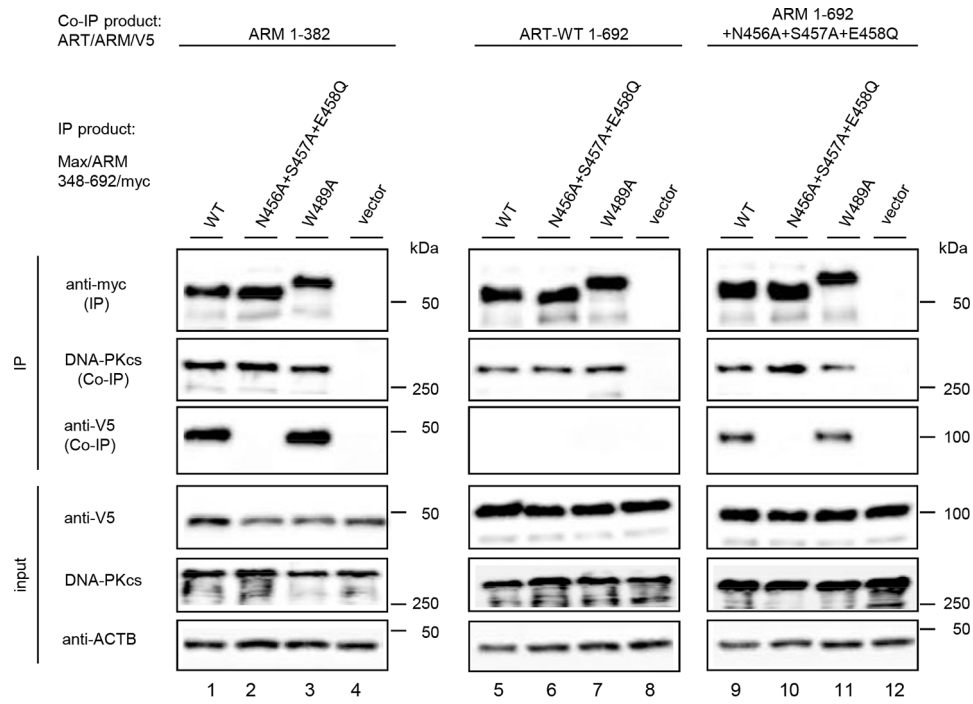

FIGURE 5. **Full-length ARTEMIS with specific mutations in the C-terminal domain and C-terminally truncated ARTEMIS have identical binding specificities with respect to the interaction with the isolated C-terminal fragment.** HEK293T cells were transfected with combinations of Myc- and V5-tagged wild type (ART-WT) or mutant (ARM) ARTEMIS-expressing plasmids as indicated. The C-terminal fragments contained either wild type sequence (*WT*) or specific amino acid exchanges as indicated *above* the lanes. Protein interactions were subsequently analyzed by Co-IP, see legend to Fig. 1 for details. Membranes were probed with anti-DNA-PKcs, anti-V5, and anti-Myc antibodies to detect Co-IP and IP products. Anti-ACTB antibody was used as loading control for input lanes. The experiment was performed twice with comparable results. Transfection efficiencies were 88–94%. The amino acid exchange W489A changes the mobility of the C-terminal fragment.

the isolated C-terminal fragment (Fig. 4, *lanes 11* and *12*), but all the others, like ART-WT, do not. Both of these mutant proteins (ARM 1–692+E454Q+S455A and ARM 1–692+N456A+S457A+E458Q) have exchanges at invariant amino acid positions within the core of the above defined C-terminal interaction domain (aa 448–462, see Fig. 1, *C* and *E*). Deletion of the 7 N-terminal amino acids in the context of the latter mutant results in loss of the interaction (ARM 8–692+N456A+S457A+E458Q, compare Fig. 4, *lanes 12* and *13*). This indicates that the observed co-immunoprecipitation indeed reflects binding to the N terminus of full-length ARTEMIS. The results illustrated in Fig. 4 are in support of the hypothesis that in ART-WT the N-terminal domain is masked by the C terminus due to self-interaction. Disabling the N-C interaction by mutation of amino acids 456–458 and to a lesser extent also of amino acids 454 + 455 (Fig. 4, *lanes 12* and *11*, respectively) liberates the N terminus of full-length ARTEMIS, which then is available for interaction with the C-terminal fragment (ARM 414–692), as demonstrated by co-immunoprecipitation.

Binding of the C-terminal Fragment to Full-length ARTEMIS and to the N-terminal Fragment Is Independent of the DNA Ligase IV Interaction Site—The experiment described in the above section was performed in CHO V-3 cells, in the absence of endogenous DNA-PKcs. Subsequent co-immunoprecipitation experiments were conducted with lysates prepared from HEK293T cells, transiently transfected with combinations of ARTEMIS expression plasmids. These experiments were optimized in two ways. First, they were performed in a reverse experimental setup, in which the V5-tagged full-length ARTEMIS protein is co-immunoprecipitated by the Myc-tagged C-terminal fragment. This increases the sensitivity of the assay, because full-length ARTEMIS is expressed much more strongly than the C-terminal fragment. Second, the C-terminal fragment was enlarged so that it contains the DNA-PKcs-binding site (*ARM 348–692,* see Fig. 1*A*) and in addition an N-terminal tag, which improves expression levels. With these modifications, co-immunoprecipitation of endogenous DNA-PKcs can be monitored as an internal control. In accordance with the results obtained in CHO V-3 cells (Fig. 4), ART-WT cannot bind the C-terminal fragment, whereas the mutant (ARM 1–692+N456A+S457A+E458Q) and the N-terminal fragment can (Fig. 5, *lanes 5, 9* and *1*, respectively). Amino acid exchanges N456A+S457A+E458Q in the immunoprecipitated C-terminal fragment abolish co-immunoprecipitation both of the N-terminal fragment and of the full-length mutant (Fig. 5, *lanes 2* and *10*) but have no effect on the DNA-PKcs interaction. Therefore, the interactions between the C-terminal fragment and the N terminus either as part of full-length ARTEMIS or as isolated fragment (ARM 1–382) have the same specificities. A DNA ligase IV interaction site in ARTEMIS (22) lies in proximity to the C-terminal domain described in this work. Therefore, we tested whether amino acid exchange W489A, which is crucial for DNA ligase IV interaction, also affected ARTEMIS self-interaction. W489A does not have an effect on the N-C interaction, neither in the context of the isolated fragments nor with respect to interaction of full-length mutant ARTEMIS (Fig. 5, *lanes 3* and *11*).

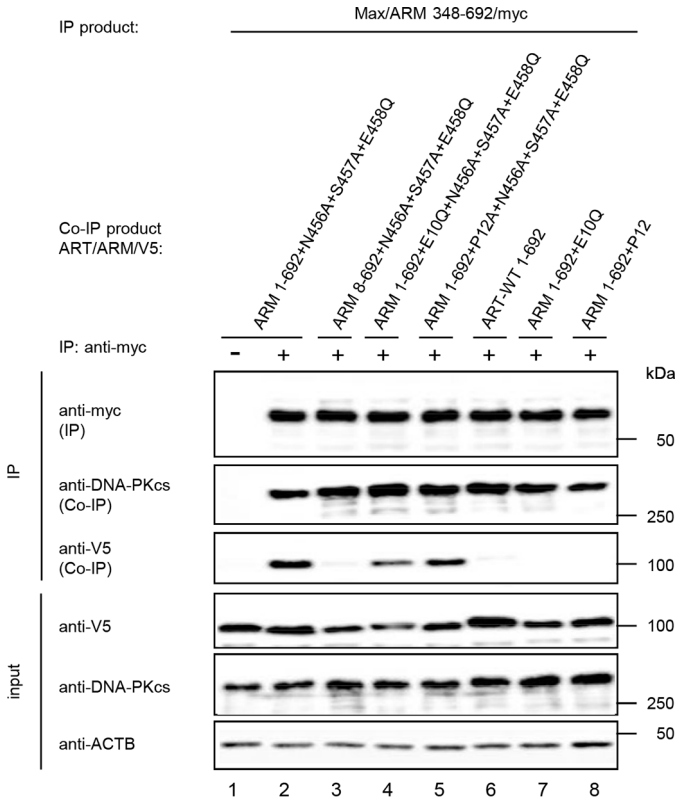

FIGURE 6. **Co-immunoprecipitation experiments with full-length ARTEMIS containing various mutations in the N- and C-terminal domains.** HEK293T cells were transfected with expression plasmids coding for Myc-tagged C-terminal fragment (Max/ARM 348–692/myc) and V5-tagged full-length ARTEMIS bearing different mutations in the N- or C-terminal regions as indicated. Protein interactions were subsequently analyzed by Co-IP, see legend to Fig. 1 for details. Membranes were probed with anti-DNA-PKcs, anti-V5, and anti-Myc antibodies to detect Co-IP and IP products. Anti-ACTB antibody was used as loading control for *input lanes*. The experiment was performed twice with comparable results. Transfection efficiencies were 87–97%.

Mutation sensitivity in the C-terminal protein binding domain is more extended, if tested in the context of the non-overlapping N- and C-terminal fragments (aa 448–462, Fig. 1*E*, *lanes 5-10*), as compared with the full-length protein (*aa 454–458,* Fig. 4, *lanes 11* and *12*). Therefore, we wanted to characterize the N-C interaction of full-length protein in more detail, in particular with respect to mutations in the N-terminal domain. In the context of the C-terminal mutation N456A+S457A+E458Q, deletion of amino acids 1–7 abolishes the interaction, whereas the single amino acid exchanges E10Q and P12A have no influence with respect to the interaction with the C-terminal fragment (Fig. 6, *lanes 1–5*). Wild type sequence in the C-terminal domain in all cases is incompatible with co-immunoprecipitation by the C terminus (Fig. 6, *lanes 6–8*).

Binding of the C-terminal Fragment to Full-length Mutant ARTEMIS Is DNA-independent—Because ARTEMIS is a nuclease, we were interested to see whether the N-C interaction is DNA-independent. We therefore performed experiments in which, prior to immunoprecipitation, the precleared lysate was incubated with ethidium bromide. By its intercalation into the DNA, ethidium bromide distorts the conformation, resulting in loss of protein-DNA interactions. The interactions of DNA-PKcs with ART-WT (17) and with KU80 (27) were used as negative and positive controls, respectively. As expected, the DNA-PKcs interaction with ART-WT (Fig. 7, *lanes 4–6*) is DNA-independent, whereas DNA-PKcs co-immunoprecipitation by KU80 is diminished in the presence of ethidium bromide, indicating its DNA dependence (Fig. 7, *lanes 7–9*). In the case of immunoprecipitation of the isolated C-terminal fragment (Max/ARM 348–692/myc), co-immunoprecipitation of both endogenous DNA-PKcs and full-length mutant ARTEMIS (ARM 1–692+N456A+S457A+E458Q) shows no difference with or without ethidium bromide (Fig. 7, *lanes 1–3*). Therefore, the newly described N-C interaction of ARTEMIS is DNA-independent.

Mutations in ARTEMIS-deficient Patients Impair the N-C Interaction of Full-length ARTEMIS—Mutations at the very N terminus of ARTEMIS abolish N-C interaction (Fig. 1*D*) and affect V(D)J recombination activity in the context of C-terminally truncated ARTEMIS (Table 1). We were interested to see the effect point mutations of ARTEMIS-deficient patients, located at various positions within the catalytic domain, have on the N-C interaction. Therefore, we tested the mutations in the context of the amino acid exchanges N456A+S457A+E458Q (Fig. 8). According to our working hypothesis, we would expect additional mutations, which destroy the N-terminal protein binding domain, to result in loss of co-immunoprecipitation by the isolated C-terminal fragment. Co-immunoprecipitation of full-length ARTEMIS is impaired in the case of proteins which contain in addition to the amino acid exchange N456A+S457A+E458Q either mutations corresponding to null alleles (G135E, D165V, and H228N (7, 28)) or amino acid exchange G211V (29) (Fig. 8, compare *lane 2* with *lanes 3, 5, 7* and *8*). Co-immunoprecipitation of full-length proteins containing in addition the hypomorphic mutations G153R and P171R (10, 11) or the polymorphism H243R (NCBI-dbSNP entry rs12768894) is clearly visible (Fig. 8, compare *lane 2* with *lanes 4, 6,* and *9*). Co-immunoprecipitation of endogenous DNA-PKcs is observed in all cases. Thus, specific mutations observed in ARTEMIS-deficient patients affect the N-C interaction in full-length proteins. Comparable results were obtained with the non-overlapping fragments (data not shown).

Mutations in ARTEMIS-deficient Patients Do Not Affect the N-N Interaction of Full-length ARTEMIS—Having demonstrated that mutations found in ARTEMIS-deficient patients have an impact on the N-C interaction (Fig. 8), we wanted to see whether the N-N interaction (see Fig. 1*B*) is also affected. We made use of the observation that additional amino acids added to the N terminus of ARTEMIS drastically reduce the N-C interaction capability (Fig. 9*A*, compare the intensities of the IP, Co-IP, and input signals). Therefore, we tested the N-N interaction of full-length ARTEMIS proteins as co-immunoprecipitation by Max/ARM 1–382/myc, which contains at its N terminus the Xpress epitope. We observe co-immunoprecipitation of all full-length proteins analyzed (Fig. 9*B*). Neither amino acid exchanges N456A+S457A+E458Q (Fig. 9*B*, *lane 2*) nor additional deletion of the 7 N-terminal amino acids (Fig. 9*B*, *lane 3*) nor single amino acid exchanges found in ARTEMIS-deficient patients (Fig. 9*B*, *lanes 4–10*) interfere with the N-N interaction. Full-length ARTEMIS protein runs at 100 kDa in SDS-

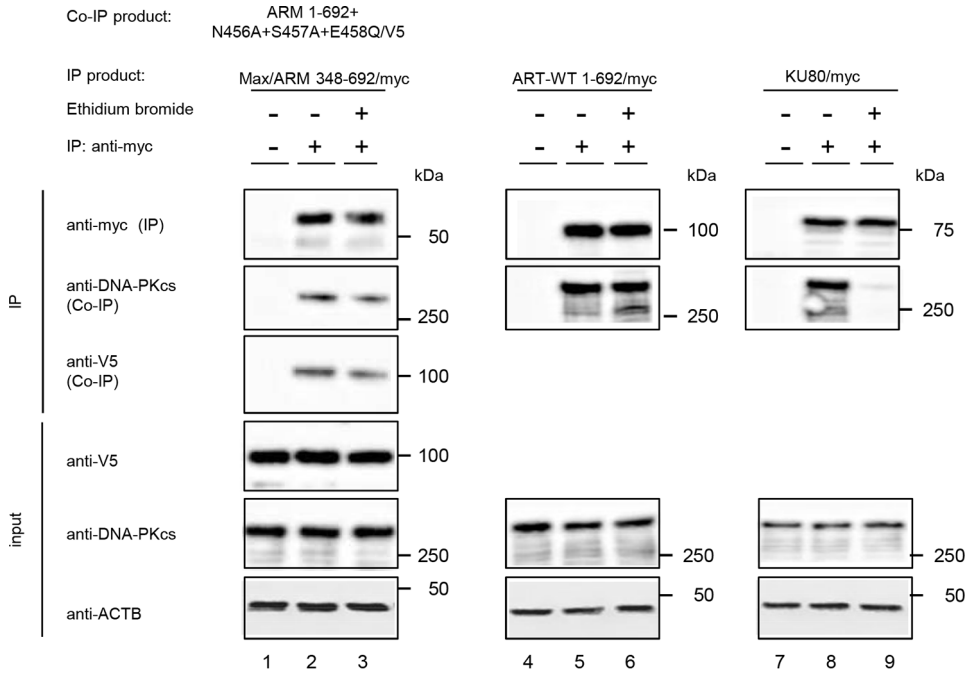

FIGURE 7. **Interaction between full-length mutant ARTEMIS and the isolated C-terminal fragment is DNA-independent.** HEK293T cells were transfected with expression plasmids coding for Myc-tagged C-terminal ARTEMIS fragment (Max/ARM 348–692/myc) in combination with V5-tagged ARTEMIS mutant ARM 1–692+N456A+S457A+E458Q (*lanes 1–3*) or for Myc-tagged ART-WT (*lanes 4–6*) or KU80 (*lanes 7–9*). Protein interactions were subsequently analyzed by Co-IP, see legend to Fig. 1 for details. Prior to immunoprecipitation with anti-Myc antibody, lysates were incubated with or without ethidium bromide as indicated. Membranes were probed with anti-DNA-PKcs (*lanes 1–9*), anti-V5 (*lanes 1–3*), and anti-Myc (*lanes 1–9*) antibodies to detect Co-IP and IP products. Anti-ACTB antibody was used as loading control for *input lanes*. The experiment was performed twice with comparable results. Transfection efficiencies were 96–99%.

PAGE. In addition, we observed a band at ~75 kDa, corresponding to a protein presumably derived from an internal translational start at position Met-121. In agreement with the differences in mutation sensitivity of the N-C *versus* N-N interactions (see Fig. 1*B*), this N-terminally truncated protein is also co-immunoprecipitated strongly via N-N interaction (Fig. 9*B, lanes 1–10*).

Expression levels of the different mutant proteins vary. In particular, proteins that have impaired N-C interaction show reduced expression levels. This also holds true for amino acid exchanges corresponding to null alleles in RS-SCID patients (G135E, D165V, and H228N), as well as amino acid exchange G211V (Fig. 9*B*, compare short exposure of input *lanes 1, 4, 6, 8,* and *9*). To evaluate the effect of the different patient mutations on protein stability in the absence of endogenous ARTEMIS, we transiently transfected the corresponding expression plasmids in ARTEMIS-deficient human primary fibroblasts and analyzed protein levels by Western blotting analysis (Fig. 10). Again, there is a dramatic reduction in expression of ARTEMIS proteins that contain amino acid exchanges corresponding to null alleles in RS-SCID patients, as well as mutation G211V (Fig. 10, *lanes 1, 3, 5,* and *6*). Because transcription in all cases is regulated by the same CMV promoter, we assume that differences in protein levels as analyzed by Western blotting reflect variations in protein stability.

ARTEMIS with Amino Acid Exchanges N546Q+S457A+E458E Is More Active than ART-WT in a Cellular V(D)J Recombination Assay—To address the question of functional relevance of the protein interaction data presented above, we performed cellular V(D)J recombination assays in ARTEMIS-deficient human primary fibroblasts. First, we established the relative expression levels of the different ARTEMIS constructs in the absence of endogenous ARTEMIS protein. We compared the expression of ART-WT and full-length ARTEMIS containing either the double amino acid exchange F446A+T447A or the triple mutation N456A+S457A+E458Q. In the co-immunoprecipitation experiments, the former mutant behaved like ART-WT, whereas the latter was shown to have an unmasked N-terminal domain (Fig. 4). Expression levels of ARM 1–692+F446A+T447A and ART-WT are comparable (Fig. 11*A*, compare *lanes 1* and *2* with *6* and *7*). However, ARM 1–692+N456A+S457A+E458Q is dramatically unstable as compared with ART-WT (Fig. 11*A*, compare *lanes 1–5* with *lane 8*). As estimated from titration of the amount of expression plasmid transfected, the expression of ARM 1–692+N456A+S457A+E458Q is reduced about 20-fold compared with ART-WT and ARM 1–692+F446A+T447A. In the subsequent cellular V(D)J recombination assay, it was important to supply ARTEMIS in limiting concentrations, to detect potential differences in the V(D)J recombination rates between wild type and mutant proteins. We therefore transfected ARTEMIS-deficient primary fibroblasts with different amounts of ARTEMIS expression vectors, keeping all other components constant and using vector without insert to fill up to identical amounts of DNA. Table 2 summarizes the results of four independent V(D)J recombination assays, each comparing the V(D)J recombination rates of ART-WT and the two mutants as well as relevant controls (−ART and −RAG1/2). The recombination rates at the different amounts of input ART/ARM expression vector (range 5–1000 ng) are similar for all three ARTEMIS

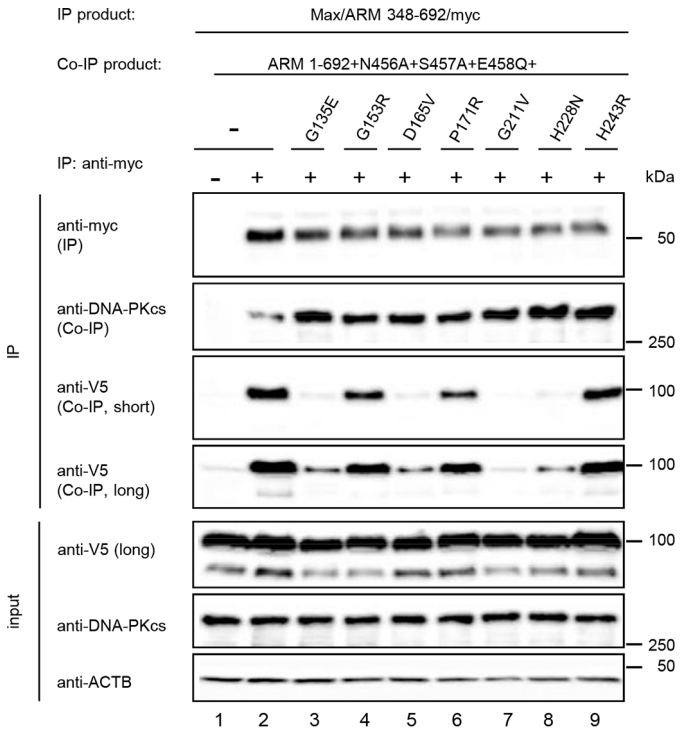

FIGURE 8. **Mutations in ARTEMIS-deficient patients affect the N-C interaction of full-length ARTEMIS.** HEK293T cells were transfected with expression plasmids coding for the Myc-tagged C-terminal fragment (Max/ARM 348–692/myc) and V5-tagged full-length protein ARM 1–692 bearing amino acid exchanges N456A+S457A+E458Q and in addition different patient mutations in the N-terminal catalytic domain as indicated *above* the corresponding lanes. Protein interactions were subsequently analyzed by Co-IP, see legend to Fig. 1 for details. Membranes were probed with anti-DNA-PKcs, anti-V5, and anti-Myc antibodies to detect Co-IP and IP products. Anti-ACTB antibody was used as loading control for *input lanes*. Two different exposure times (*short, long*) are shown for detection of the Co-IP with anti-V5 antibody. The experiment was performed twice with comparable results. Transfection efficiencies were 95–97%.

proteins (Table 2 and Fig. 11*B*). Taking into account the difference in expression levels (Fig. 11*A*) and presuming that a similar ratio is also present in the cellular V(D)J recombination assay, ARM 1–692+N456A+S457A+E458Q is much more active than ART-WT and mutant ARM 1–692+F446A+T447A. Fig. 11*C* illustrates the relative V(D)J recombination activities if a 10-fold difference in expression levels at ARTEMIS-limiting conditions is assumed. In this case, ARM 1–692+N456A+S457A+E458Q is 4.5-fold more active in V(D)J recombination than ART-WT. Expression levels at the 5- and 50-ng input of the corresponding expression vectors are far below the detection limit of Western blotting analyses, precluding this control. The results of the cellular V(D)J recombination assays, comparing ART-WT to full-length ARTEMIS with specific mutations within the C-terminal protein binding domain (Table 2 and Fig. 11), are in support of the hypothesis that ARTEMIS function is regulated by autoinhibition via the C-terminal domain.

Phosphomimetic Amino Acid Exchanges in C-terminal ATM and DNA-PKcs Phosphorylation Sites Do Not Unmask the Catalytic Domain—ARTEMIS with amino acid exchanges N546Q+S457A+E458E, which abolish the intrinsic N-C interaction, is a useful experimental tool, mimicking activation of ARTEMIS function. We wanted to assess whether phosphorylation of the C terminus affects the interaction between the N- and C-terminal domains. In full-length ARTEMIS we introduced phosphomimetic amino acid exchanges (Ser to Glu) at one or more previously described phosphorylation sites (16, 18, 19, 25). As depicted in Fig. 12, only the positive control (ARM 1–692+N546Q+S457A+E458E, *lane 2*), but none of the other full-length ARTEMIS proteins, can be co-immunoprecipitated by the C-terminal fragment. Thus, constitutive negative charge provided by glutamic acid at positions 503, 516, 534, 538, 562, 645, and 656 in the ARTEMIS C-terminal tail does not affect the accessibility of the N terminus in full-length ARTEMIS, as monitored by co-immunoprecipitation.

Discussion

Protein crystallography is a potent technique for the analysis of conformational changes in proteins and has been successfully employed for DNA-PKcs and other enzymes of the NHEJ pathway (30). However, until now, no structural data were available for full-length ARTEMIS. We therefore conducted co-immunoprecipitation experiments to test whether ARTEMIS is capable of self-interaction, a prerequisite for autoinhibition mediated by protein-protein interaction (31). Our experiments with ARTEMIS fragments identify protein binding domains that mediate two independent modes of self-interaction as follows: the N-C interaction between non-overlapping fragments from the N- and C-terminal portions of ARTEMIS and the N-N interaction in which the N-terminal domain binds to itself. Systematic analyses with different combinations of full-length ARTEMIS proteins and N- or C-terminal fragments allow the following conclusions. (*a*) In wild type ARTEMIS the N terminus is engaged with binding to the C-terminal domain. (*b*) Specific mutations in the C-terminal domain of full-length protein (aa 454–458) abolish this interaction, leaving the N terminus free to bind the isolated C-terminal fragment. These results suggest that mutant ARM 1–692+N456A+S457A+E458Q adopts a different conformation than ART-WT. Evidence is strong that the N-C interaction of full-length ARTEMIS corresponds to the interaction observed between the non-overlapping N- and C-terminal fragments, because deletion of the 7 N-terminal amino acids abolishes binding in either case. Importantly, the N-C interaction is DNA-independent. In the N-terminal protein binding domain amino acid exchanges in conserved residues distributed throughout the metallo-β-lactamase and β-CASP domains are important for the N-C interaction. This resembles the mutation sensitivity observed in V(D)J recombination assays performed to define the catalytic center of the nuclease (5, 6). In this study, we show that in the context of C-terminally truncated ARTEMIS deletion of and missense mutations in the N terminus result in loss of both V(D)J recombination activity and N-C interaction. Interestingly, amino acid exchange P12A allows a separation of functions, because it impairs V(D)J recombination activity but retains N-C interaction capability.

The majority of missense mutations found in patients diagnosed with an ARTEMIS defect lie in the N-terminal catalytic domain (7). In this study, we show that mutations found in ARTEMIS-deficient patients affect the N-C but not the N-N interaction. These results also suggest that in full-length ARTEMIS the N-C interaction and the concomitant masked confor-

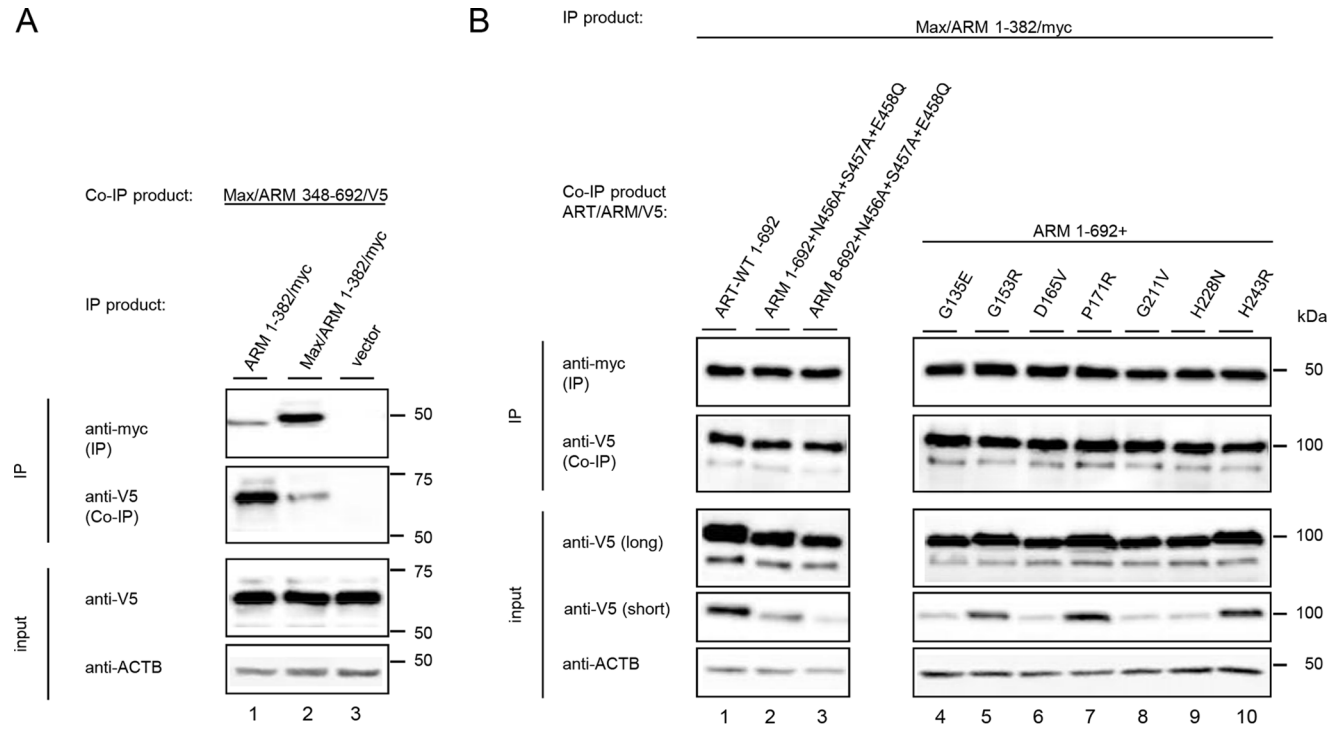

FIGURE 9. **Mutations in ARTEMIS-deficient patients have no effect on the N-N interaction of full-length ARTEMIS.** HEK293T cells were transfected with combinations of ARTEMIS expression plasmids as indicated, and Co-IP experiments were performed. See legend to Fig. 1 for details. Membranes were probed with anti-DNA-PKcs, anti-V5, and anti-Myc antibodies to detect Co-IP and IP products. Anti-ACTB antibody was used as loading control for *input lanes*. *A,* N-C interaction of the N-terminal fragment with (Max/ARM 1–382/myc) or without (ARM 1–382/myc) an N-terminal Xpress epitope. The experiment was performed twice with comparable results. Transfection efficiencies were 92–95%. *B,* N-N interaction of full-length ARTEMIS bearing different mutations as indicated *above* the corresponding lanes. Two different exposure times (*short, long*) are shown for detection of input with anti-V5 antibody. The experiment was performed twice with comparable results. Transfection efficiencies were 82–87%.

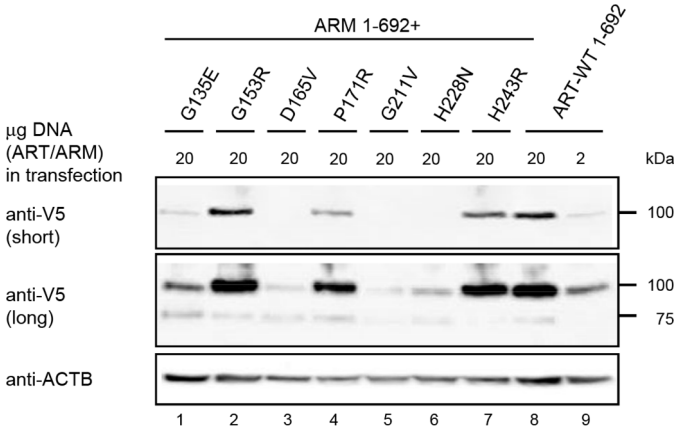

FIGURE 10. **Expression of mutant full-length ARTEMIS proteins in ARTEMIS-deficient human primary skin fibroblasts.** ARTEMIS-deficient human primary skin fibroblasts were transfected with the indicated amounts of expression plasmids coding for wild type (ART-WT) or full-length mutant ARTEMIS. The specific amino acid exchanges in the N terminus are indicated *above* the corresponding lanes. Equal amounts of cell lysates were analyzed by SDS-PAGE and Western blotting. Two different exposure times (*short, long*) are shown for detection of ART-WT/ARM proteins with anti-V5 antibody. Anti-ACTB antibody was employed as loading control. The position of protein standards is given at the *right* in kDa. The experiment was performed twice with comparable results. Transfection efficiencies were 71–77%.

mation are not a prerequisite for the N-N interaction. Amino acid exchanges corresponding to null alleles (G135E, D165V, and H228N) and G211V but not the hypomorphic mutations G153R and P171R impair N-C interaction. Notably, in full-length context mutations corresponding to null alleles in ARTEMIS-deficient patients result in reduced expression of the respective proteins as compared with ART-WT. The coincidence of reduced expression levels and loss of N-C interaction of full-length proteins may point to a causal relationship. Therefore, we tentatively suggest that mutations that inactivate the N-C interaction destabilize the protein, and this is also contributing to the RS-SCID phenotype. In principle, the N-C interaction of full-length protein and protein stabilization could occur either as an inter- or intramolecular event, and both possibilities are compatible with the data presented. Unfortunately, the overlapping association via the N-N interaction, as well as the fact that additional amino acids positioned at the N terminus impair the N-C interaction, precludes simple experiments from answering this important question. Until now, we have not been able to identify any single amino acid mutation affecting the N-N interaction, and analyses with many different deletion constructs suggest that this interaction is mediated by several redundant interfaces (data not shown).

C-terminally truncated ARTEMIS is sufficient to confer V(D)J recombination activity (5, 21). Here we show that amino acid exchanges N456A+S457A+E458Q, which abolish N-C interaction, result in a 4.5-fold increase in V(D)J recombination activity as compared with ART-WT. Similar results were shown for ARM 1–382 and were also obtained with C-terminally truncated ARM 1–413 (data not shown). Therefore, we would like to conclude that a conformational change occurs during activation of ARTEMIS, involving loss of physical association between the N- and C-terminal parts of the protein. This provides conclusive evidence for the formerly postulated

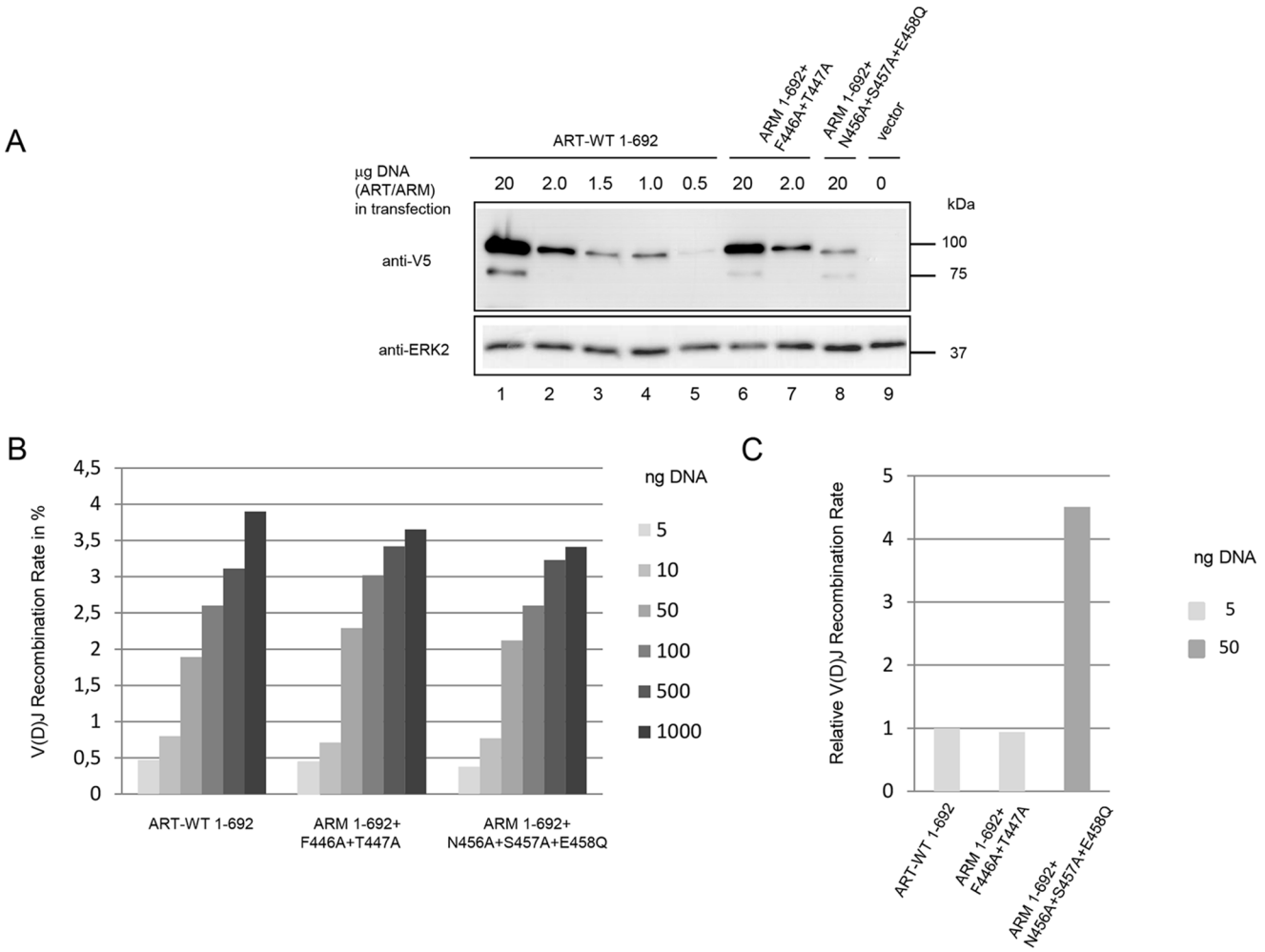

FIGURE 11. **Specific mutations in the C-terminal domain result in increased V(D)J recombination activity.** *A,* ARTEMIS-deficient human primary skin fibroblasts were transfected with the designated amounts of expression plasmids coding for wild type (ART-WT 1–692) or full-length mutant ARTEMIS, supplemented with vector DNA. The specific amino acid exchanges in the C terminus are indicated. Equal amounts of cell lysates were analyzed by SDS-PAGE and Western blotting; anti-V5 antibody was used to detect ART-WT/ARM proteins, and antibody directed against extracellular signal-regulated kinase 2 (ERK2) was employed as loading control. The position of protein standards is given at the *right* in kDa. Transfection efficiencies were 79–94%. *B* and *C,* graphic representation of the results from V(D)J recombination assays in ARTEMIS-deficient human primary skin fibroblasts. V(D)J recombination rates correspond to the means of four independent experiments (see Table 2). *B,* V(D)J recombination rates with titration (5–1000 ng) of plasmids expressing ART/ARM proteins as indicated. *C,* comparison of V(D)J recombination rates with ART/ARM proteins in limiting amounts and taking into account a 10-fold difference in expression as estimated from *A*. The V(D)J recombination rate of ART-WT 1–692 at 5 ng of input expression plasmid was set to 1 and compared with the V(D)J recombination rates of ARM 1–692+F446A+T447A and ARM 1–692+N456A+S457A+E458Q at 5 and 50 ng of input expression plasmids, respectively.

TABLE 2

V(D)J recombination assay in ARTEMIS-deficient human primary skin fibroblasts complemented with ARTEMIS mutants containing amino acid exchanges in the C-terminal interaction region

Human primary skin fibroblasts were co-transfected with V(D)J recombination plasmid and plasmids expressing RAG1, RAG2, and one of the ARTEMIS proteins (wild type or mutant). As negative controls, the same co-transfections without the plasmids expressing RAG2 (−RAG2) or wild type ARTEMIS (−ART) were performed. ART-WT/ARM expression plasmids were titrated (5, 10, 50, 100, 500, and 1000 ng) and supplemented with vector plasmid. In each assay 5×10^4 fibroblasts were analyzed by FACS analysis. The percentages of recombination-positive cells out of the subpopulation of transfected fibroblasts are shown.

	Controls								+ART-WT 1–692				+ARM 1–692+ F446A+T447A				+ARM 1–692+ N456A+S457A+ E458Q			
	−RAG1				−ART															
pcDNA6 ART/ARM	A	B	C	D	A	B	C	D	A	B	C	D	A	B	C	D	A	B	C	D
ng																				
1000	0.14	0.08	0.10	0.09	0.12	0.14	0.09	0.08	4.96	4.65	3.96	2.47	4.15	4.32	4.06	2.50	3.34	4.46	3.73	2.55
500									2.69	4.12	3.67	2.41	2.69	4.38	4.39	2.65	2.16	4.33	4.18	2.68
100									3.05	2.87	3.12	1.79	2.97	3.67	3.79	2.10	2.70	2.86	3.33	1.96
50									1.86	1.92	2.74	1.48	2.20	2.86	2.84	1.71	2.72	2.43	2.21	1.56
10									0.75	1.22	0.96	0.69	0.70	0.90	1.08	0.59	0.73	0.63	1.48	0.67
5									0.55	0.64	0.76	0.37	0.43	0.71	0.62	0.42	0.42	0.47	0.74	0.34

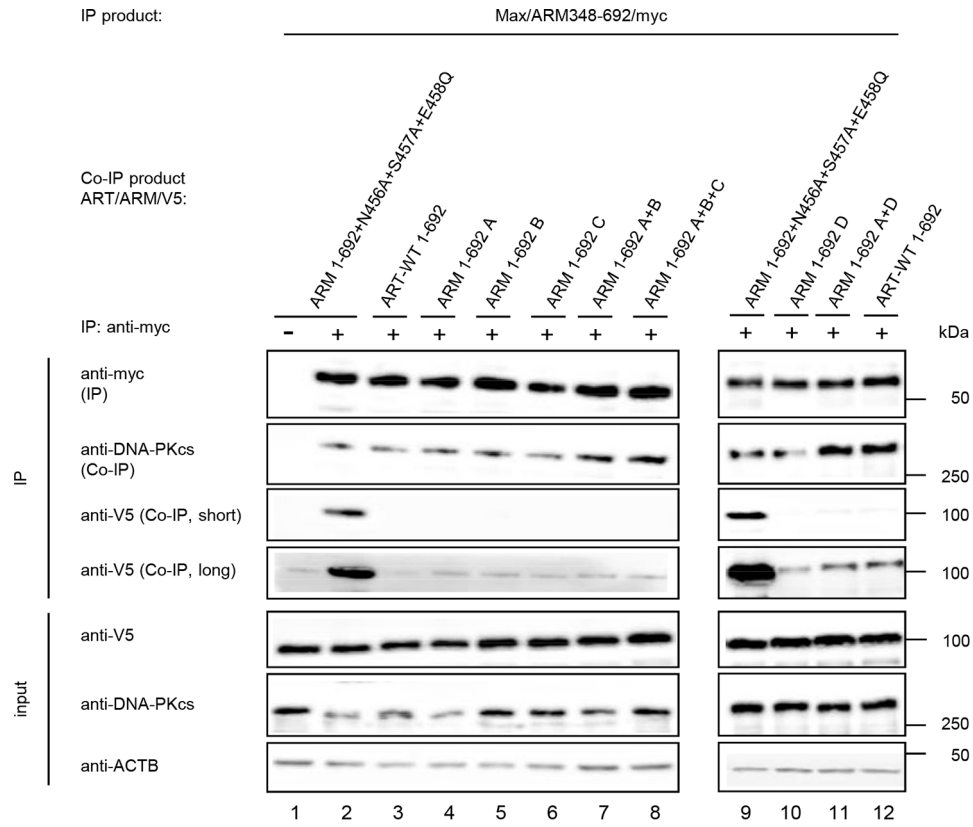

FIGURE 12. **Phosphomimetic amino acid exchanges in DNA-PKcs and ATM phosphorylation sites do not unmask the N terminus of full-length ARTEMIS.** HEK293T cells were transfected with expression plasmids coding for the Myc-tagged C-terminal fragment (*Max/ARM 348–692*/myc) and V5-tagged full-length ARTEMIS (*ART-WT/ARM 1-692*) bearing different phosphomimetic amino acid exchanges in C-terminal phosphorylation sites (*A,* S645E; *B,* S503E+S516E; *C,* S534E+S538E+S562E; and *D,* T656E). Protein interactions were subsequently analyzed by Co-IP, see legend to Fig. 1 for details. Membranes were probed with anti-DNA-PKcs, anti-V5, and anti-Myc antibodies to detect Co-IP and IP products. Anti-ACTB antibody was used as loading control for *input lanes*. Two different exposure times (*short, long*) are shown for detection of the Co-IP product with anti-V5 antibody. The experiment was performed twice with comparable results. Transfection efficiencies were 91–97%.

autoinhibition model (15, 21). *In vitro* nuclease assays with purified components are potent experiments for the analysis of ARTEMIS function. It will be of interest to elucidate the effect of amino acid exchanges N456A+S457A+E458Q on the different endo- and exonucleolytic activities of ARTEMIS and in particular their dependence on the presence of and the phosphorylation by DNA-PKcs. However, mutations N456A+S457A+E458Q are only an experimental model imitating the activation process, and it will be of utmost interest to identify the physiological stimuli, inducing the postulated conformational change. Post-translational modifications and the displacement of inhibitory domains by intermolecular interactions with activator proteins are frequent mechanisms for the relief of autoinhibition (31). A well studied example is the Wiskott-Aldrich syndrome protein family, which includes proteins that regulate actin assembly (32). Loss of Wiskott-Aldrich syndrome protein function results in immunodeficiency (33). Autoinhibition is mediated by an intramolecular interaction, and activation involves binding of regulatory proteins to the inhibitory domain and phosphorylation (32, 34). In ARTEMIS, DNA ligase IV binds to the C-terminal tail (22) in the vicinity of the protein binding domain described in this work. Mutation of the DNA ligase IV-binding site in ARTEMIS did not affect the N-C interaction, indicating that DNA ligase IV is not a mediator. Specific mutations in the N-terminal fragment impair both N-C interaction and V(D)J recombination activity. Therefore, we assume that the activation step most likely affects either the C-terminal domain itself or amino acids that link it to the N-terminal catalytic domain. The first possibility is underscored by our finding that the N-C interactions of full-length protein and of non-overlapping fragments are comparable with respect to mutation sensitivity in both protein binding domains. Mutations N456A+S457A+E458Q hit residues that can form salt and amide bridges, and this may either distort protein folding or affect directly the interaction surface in the C-terminal protein binding domain.

Phosphorylation by DNA-PKcs is not a prerequisite for ARTEMIS self-interaction, because our initial experiments were conducted in CHO-V3 cells. Also, an intact DNA-PKcs binding domain in ARTEMIS is dispensable. The C-terminal domain (aa 454–458) contains a stretch of predominantly acidic residues and in addition three serines which, upon phosphorylation, could add to the overall negative charge. However, these serines do not correspond to consensus phosphorylation sites (35). *In vitro* Ser-503, Ser-516, and Ser-645 in ARTEMIS have been defined as major DNA-PKcs and/or ATM phosphorylation sites (16), but other serines and threonines are also phosphorylated (15, 17). Importantly, Ser-645 in ARTEMIS is phosphorylated *in vivo* in an ATM-dependent manner, and induction of DNA DSB by IR leads to hyperphosphorylation at

this site (16, 19). Phosphorylation at Ser-645 and Thr-656 is important for ATM-dependent association between ARTEMIS and PTIP (25). Here, we show that phosphomimetic mutations at seven sites (S503E, S516E, S534E, S538E, S562E, S645E, and T656E) do not affect N-C interaction in full-length ARTEMIS. Although it cannot be excluded that glutamic acid was insufficient in mimicking phosphorylation, our results have not provided evidence that phosphorylation at the sites tested is the *in vivo* trigger, which leads to unmasking of the N-terminal catalytic domain. DNA-PKcs autophosphorylation has been implicated in the regulation of ARTEMIS endonucleolytic activities, and it is assumed that the precise positioning of the nuclease on different DNA substrates is crucially regulated by the phosphorylation status of the kinase (16, 36). The importance of the ARTEMIS/DNA-PKcs interplay is apparent also from the first DNA-PKcs-deficient RS-SCID patient described (37). The patient phenotype closely resembles that of RS-SCID patients with ARTEMIS null mutations possibly reflecting impairment of ARTEMIS activation by DNA-PKcs. Additional experiments will have to be performed to address the question how ARTEMIS self-interaction and the relief of autoinhibition are related to phosphorylation by DNA-PKcs. Clearly, C-terminally truncated ARTEMIS is a very potent interaction partner of DNA-PKcs (21).

The involvement of DNA repair factors in tumorigenesis is well established for some and speculative for others (38). In the case of ARTEMIS, a hypomorphic allele found in CID patients and resulting in a C-terminally truncated protein was suspected to predispose to lymphoma (8). Analyses in mice provided evidence that the corresponding mutation leads to genomic instability and, in the absence of p53, to enhanced tumorigenesis (39, 40). Intriguingly, this mutation results in a frameshift at position Asp-451, followed by translational termination 10 residues to the C terminus. Thus the C-terminal truncation leaves the DNA-PKcs binding region intact but destroys the C-terminal self-interaction domain described in this study (aa 454–458). Overexpression of wild type ARTEMIS in mice does not lead to lymphopoietic malignancies (41). Therefore, we cautiously speculate that loss of the N-C interaction, resulting in an unmasked catalytic domain, may possibly cause DNA instability. In diffuse large B cell lymphomas, DNA repair genes are selectively mutated, and the somatic mutation identified in ARTEMIS also resulted in a C-terminally truncated protein (42). DNA repair factors have been in special focus for the development of novel strategies for the treatment of drug-resistant tumors (26). The findings presented in this study, describing a protein interaction interphase involved in the activation of the structure-specific nuclease ARTEMIS, may help to refine the search for small molecular compounds that specifically block this activation.

In summary, we have presented evidence that a physical interaction between the N-terminal catalytic domain and the C-terminal tail of the ARTEMIS protein mediates the previously postulated autoinhibition of the nuclease. Specific amino acid exchanges in the C-terminal protein binding domain result in a conformational change that unmasks the N terminus and results in increased V(D)J recombination activity. Phosphomimetic mutations in the C-terminal domain did not induce the postulated conformational change, so the exact role of DNA-PKcs in the relief of autoinhibition still needs to be elucidated. Mutations found in ARTEMIS-deficient patients and contained in the catalytic domain affect the interaction with the C-terminal domain and possibly, as a consequence, also protein stability.

Experimental Procedures

Cells and Transfections—HEK293T cells were cultured in DMEM supplemented with 10% FCS and transfected using the calcium phosphate precipitation method. Human primary ARTEMIS-deficient skin fibroblasts were cultured in IMDM, supplemented with 10% FCS, and transfected by nucleofection (Amaxa^{TM} Cell line Nucleofector Kit V, Lonza). The DNA-PKcs negative CHO cell line V-3 was cultured in IMDM supplemented with 10% FCS and transfected by nucleofection (Amaxa^{TM} Cell line Nucleofector Kit T, Lonza). In transfections with DNA titrations, the total amount of DNA was kept constant with vector DNA.

Protein Expression Constructs—Human wild type (ART-WT) and mutant (ARM) ARTEMIS expression plasmids were cloned via KpnI/NotI restriction sites into pcDNA6myc-His and pcDNA6V5-His vector (Invitrogen, Breda, Netherlands). The nomenclature refers to the amino acids included in the respective ARTEMIS mutant proteins (ARM). Construct ARM 8–692 corresponds to ARM29 in Ref. 9, and constructs ARM 1–413 and ARM 1–382 correspond to ARM37 and ARM23 in Ref. 21. The supplemental Table 1 shows the forward and reverse primers used for amplification of the ARTEMIS cDNAs of the deletion mutants. In expression plasmids Max/ARM 348–692/myc and Max/ARM 1–382/myc the ARTEMIS cDNAs were cloned via KpnI and NotI into pcDNA4His/Max vector (Invitrogen), which in addition contained at the C terminus the Myc fusion tag, derived from pcDNA6myc-His (Invitrogen). Mutations corresponding to specific amino acid exchanges were introduced using either the QuikChange Site-Directed Mutagenesis kit (Agilent Technologies) or the NEBuilder^{TM} HiFi DNA assembly cloning kit (New England Biolabs). Primers used for mutagenesis are given in supplemental Table 2. Subsequent to cloning, all ARTEMIS ORFs of the corresponding plasmids were confirmed by sequencing.

Immunoprecipitation Assay and Immunoblotting—The immunoprecipitation assay was performed essentially as described (2) with some modifications. Prior to immunoprecipitation with anti-Myc antibody (Life Technologies, Inc.), a preclearing step with protein G-Sepharose was performed. Experiments depicted in Figs. 5–9 and 12 were performed using 100 mM KCl. To determine the DNA independence of protein-protein interactions, precleared lysates were incubated 30 min on ice with or without ethidium bromide (200 μg/ml), followed by 5 min of centrifugation. The supernatant was used in standard immunoprecipitation assays. Endogenous DNA-PKcs was detected using polyclonal anti-DNA-PKcs antibody (ab69527, Abcam). Myc- and V5-tagged ARTEMIS Proteins were detected with anti-Myc and anti-V5 antibodies (Life Technologies, Inc., catalog nos. 46-1155 and 46-1157). Antibodies directed against ACTB (Abcam, ab8227), ERK2 (Santa Cruz, sc-1647), and HPRT (Abcam, ab10479) were used as loading control.

V(D)J Recombination Assay—The cellular V(D)J recombination assay and FACS analyses of transfected human primary ARTEMIS-negative fibroblasts were carried out as described (6). For titration of ARTEMIS expression vectors, the total DNA content was kept constant, using vector DNA without insert.

Author Contributions—D. N. and K. S. designed the study and analyzed results. D. N., I. P., and C. B. were responsible for experimental data. D. N. prepared the initial draft of the manuscript. All authors contributed to the discussion and the preparation of the final version of the manuscript.

Acknowledgments—We acknowledge U. Pannicke for discussions and critical reading of the manuscript and T. Gebauer and E. Rump for providing plasmids containing ARTEMIS mutations G135E, G153R, P171R, H228N, and H243R.

References

1. Moshous, D., Callebaut, I., de Chasseval, R., Corneo, B., Cavazzana-Calvo, M., Le Deist, F., Tezcan, I., Sanal, O., Bertrand, Y., Philippe, N., Fischer, A., and de Villartay, J. P. (2001) Artemis, a novel DNA double-strand break repair/V(D)J recombination protein, is mutated in human severe combined immune deficiency. *Cell* **105,** 177–186
2. Ma, Y., Pannicke, U., Schwarz, K., and Lieber, M. R. (2002) Hairpin opening and overhang processing by an Artemis/DNA-dependent protein kinase complex in nonhomologous end joining and V(D)J recombination. *Cell* **108,** 781–794
3. Lieber, M. R. (2010) The mechanism of double-strand DNA break repair by the nonhomologous DNA end-joining pathway. *Annu. Rev. Biochem.* **79,** 181–211
4. Callebaut, I., Moshous, D., Mornon, J.-P., and de Villartay, J.-P. (2002) Metallo-β-lactamase fold within nucleic acids processing enzymes: the β-CASP family. *Nucleic Acids Res.* **30,** 3592–3601
5. Poinsignon, C., Moshous, D., Callebaut, I., de Chasseval, R., Villey, I., and de Villartay, J.-P. (2004) The metallo-β-lactamase/β-CASP domain of Artemis constitutes the catalytic core for V(D)J recombination. *J. Exp. Med.* **199,** 315–321
6. Pannicke, U., Ma, Y., Hopfner, K.-P., Niewolik, D., Lieber, M. R., and Schwarz, K. (2004) Functional and biochemical dissection of the structure-specific nuclease ARTEMIS. *EMBO J.* **23,** 1987–1997
7. Pannicke, U., Hönig, M., Schulze, I., Rohr, J., Heinz, G. A., Braun, S., Janz, I., Rump, E.-M., Seidel, M. G., Matthes-Martin, S., Soerensen, J., Greil, J., Stachel, D. K., Belohradsky, B. H., Albert, M. H., *et al.* (2010) The most frequent DCLRE1C (ARTEMIS) mutations are based on homologous recombination events. *Hum. Mutat.* **31,** 197–207
8. Moshous, D., Pannetier, C., Chasseval, Rd. Rd., Deist, Fl. Fl., Cavazzana-Calvo, M., Romana, S., Macintyre, E., Canioni, D., Brousse, N., Fischer, A., Casanova, J.-L., and Villartay, J.-P. de (2003) Partial T and B lymphocyte immunodeficiency and predisposition to lymphoma in patients with hypomorphic mutations in Artemis. *J. Clin. Invest.* **111,** 381–387
9. Ege, M., Ma, Y., Manfras, B., Kalwak, K., Lu, H., Lieber, M. R., Schwarz, K., and Pannicke, U. (2005) Omenn syndrome due to ARTEMIS mutations. *Blood* **105,** 4179–4186
10. Lagresle-Peyrou, C., Benjelloun, F., Hue, C., Andre-Schmutz, I., Bonhomme, D., Forveille, M., Beldjord, K., Hacein-Bey-Abina, S., De Villartay, J.-P., Charneau, P., Durandy, A., Fischer, A., and Cavazzana-Calvo, M. (2008) Restoration of human B-cell differentiation into NOD-SCID mice engrafted with gene-corrected $CD34^+$ cells isolated from Artemis or RAG1-deficient patients. *Mol. Ther.* **16,** 396–403
11. Woodbine, L., Grigoriadou, S., Goodarzi, A. A., Riballo, E., Tape, C., Oliver, A. W., van Zelm, M. C., Buckland, M. S., Davies, E. G., Pearl, L. H., and Jeggo, P. A. (2010) An Artemis polymorphic variant reduces Artemis activity and confers cellular radiosensitivity. *DNA Repair* **9,** 1003–1010
12. Li, S., Chang, H. H., Niewolik, D., Hedrick, M. P., Pinkerton, A. B., Hassig, C. A., Schwarz, K., and Lieber, M. R. (2014) Evidence that the DNA endonuclease ARTEMIS also has intrinsic 5′-exonuclease activity. *J. Biol. Chem.* **289,** 7825–7834
13. Riballo, E., Kühne, M., Rief, N., Doherty, A., Smith, G. C., Recio, M.-J., Reis, C., Dahm, K., Fricke, A., Krempler, A., Parker, A. R., Jackson, S. P., Gennery, A., Jeggo, P. A., and Löbrich, M. (2004) A pathway of double-strand break rejoining dependent upon ATM, Artemis, and proteins locating to γ-H2AX foci. *Mol. Cell* **16,** 715–724
14. Zhang, X., Succi, J., Feng, Z., Prithivirajsingh, S., Story, M. D., and Legerski, R. J. (2004) Artemis is a phosphorylation target of ATM and ATR and is involved in the G_2/M DNA damage checkpoint response. *Mol. Cell. Biol.* **24,** 9207–9220
15. Ma, Y., Pannicke, U., Lu, H., Niewolik, D., Schwarz, K., and Lieber, M. R. (2005) The DNA-dependent protein kinase catalytic subunit phosphorylation sites in human Artemis. *J. Biol. Chem.* **280,** 33839–33846
16. Goodarzi, A. A., Yu, Y., Riballo, E., Douglas, P., Walker, S. A., Ye, R., Härer, C., Marchetti, C., Morrice, N., Jeggo, P. A., and Lees-Miller, S. P. (2006) DNA-PK autophosphorylation facilitates Artemis endonuclease activity. *EMBO J.* **25,** 3880–3889
17. Soubeyrand, S., Pope, L., De Chasseval, R., Gosselin, D., Dong, F., de Villartay, J.-P., and Haché, R. J. (2006) Artemis phosphorylated by DNA-dependent protein kinase associates preferentially with discrete regions of chromatin. *J. Mol. Biol.* **358,** 1200–1211
18. Poinsignon, C., de Chasseval, R., Soubeyrand, S., Moshous, D., Fischer, A., Haché, R. J., and de Villartay, J.-P. (2004) Phosphorylation of Artemis following irradiation-induced DNA damage. *Eur. J. Immunol.* **34,** 3146–3155
19. Chen, L., Morio, T., Minegishi, Y., Nakada, S.-I., Nagasawa, M., Komatsu, K., Chessa, L., Villa, A., Lecis, D., Delia, D., and Mizutani, S. (2005) Ataxia-telangiectasia-mutated dependent phosphorylation of Artemis in response to DNA damage. *Cancer Sci.* **96,** 134–141
20. Wang, J., Pluth, J. M., Cooper, P. K., Cowan, M. J., Chen, D. J., and Yannone, S. M. (2005) Artemis deficiency confers a DNA double-strand break repair defect and Artemis phosphorylation status is altered by DNA damage and cell cycle progression. *DNA Repair* **4,** 556–570
21. Niewolik, D., Pannicke, U., Lu, H., Ma, Y., Wang, L.-C., Kulesza, P., Zandi, E., Lieber, M. R., and Schwarz, K. (2006) DNA-PKcs dependence of Artemis endonucleolytic activity, differences between hairpins and 5′ or 3′ overhangs. *J. Biol. Chem.* **281,** 33900–33909
22. Malu, S., De Ioannes, P., Kozlov, M., Greene, M., Francis, D., Hanna, M., Pena, J., Escalante, C. R., Kurosawa, A., Erdjument-Bromage, H., Tempst, P., Adachi, N., Vezzoni, P., Villa, A., Aggarwal, A. K., and Cortes, P. (2012) Artemis C-terminal region facilitates V(D)J recombination through its interactions with DNA Ligase IV and DNA-PKcs. *J. Exp. Med.* **209,** 955–963
23. De Ioannes, P., Malu, S., Cortes, P., and Aggarwal, A. K. (2012) Structural basis of DNA ligase IV-Artemis interaction in nonhomologous end-joining. *Cell Rep.* **2,** 1505–1512
24. Ochi, T., Gu, X., and Blundell, T. L. (2013) Structure of the catalytic region of DNA ligase IV in complex with an Artemis fragment sheds light on double-strand break repair. *Structure* **21,** 672–679
25. Wang, J., Aroumougame, A., Lobrich, M., Li, Y., Chen, D., Chen, J., and Gong, Z. (2014) PTIP associates with Artemis to dictate DNA repair pathway choice. *Genes Dev.* **28,** 2693–2698
26. Furgason, J. M., and Bahassi el, M. (2013) Targeting DNA repair mechanisms in cancer. *Pharmacol. Ther.* **137,** 298–308
27. Suwa, A., Hirakata, M., Takeda, Y., Jesch, S. A., Mimori, T., and Hardin, J. A. (1994) DNA-dependent protein kinase (Ku protein-p350 complex) assembles on double-stranded DNA. *Proc. Natl. Acad. Sci. U.S.A.* **91,** 6904–6908
28. Noordzij, J. G., Verkaik, N. S., van der Burg, M., van Veelen, L. R., de Bruin-Versteeg, S., Wiegant, W., Vossen, J. M., Weemaes, C. M., de Groot, R., Zdzienicka, M. Z., van Gent, D. C., and van Dongen, J. J. (2003) Radiosensitive SCID patients with Artemis gene mutations show a complete B-cell differentiation arrest at the pre-B-cell receptor checkpoint in bone marrow. *Blood* **101,** 1446–1452
29. Perez-Becker Niehuis, T.,Perez-Becker Niehuis, T., Siepermann, K., Pannicke, U., and Schwarz K. (2009) *26th Annual Meeting of the Arbeitsgemeinschaft Pädiatrische Immunologie* (*API*), *Ittingen, Germany, May 15–17, 2009,* API, Aachen, Germany

30. Ochi, T., Wu, Q., and Blundell, T. L. (2014) The spatial organization of non-homologous end joining: from bridging to end joining. *DNA Repair* **17,** 98–109
31. Pufall, M. A., and Graves, B. J. (2002) Autoinhibitory domains: modular effectors of cellular regulation. *Annu. Rev. Cell Dev. Biol.* **18,** 421–462
32. Massaad, M. J., Ramesh, N., and Geha, R. S. (2013) Wiskott-Aldrich syndrome: a comprehensive review. *Ann. N.Y. Acad. Sci.* **1285,** 26–43
33. Derry, J. M., Ochs, H. D., and Francke, U. (1994) Isolation of a novel gene mutated in Wiskott-Aldrich syndrome. *Cell.* **78,** 635–644
34. Kim, A. S., Kakalis, L. T., Abdul-Manan, N., Liu, G. A., and Rosen, M. K. (2000) Autoinhibition and activation mechanisms of the Wiskott-Aldrich syndrome protein. *Nature* **404,** 151–158
35. Baretić, D., and Williams, R. L. (2014) PIKKs–the solenoid nest where partners and kinases meet. *Curr. Opin. Struct. Biol.* **29,** 134–142
36. Chang, H. H., and Lieber, M. R. (2016) Structure-specific nuclease activities of Artemis and the Artemis: DNA-PKcs complex. *Nucleic Acids Res.* **44,** 4991–4997
37. van der Burg, M., Ijspeert, H., Verkaik, N. S., Turul, T., Wiegant, W. W., Morotomi-Yano, K., Mari, P.-O., Tezcan, I., Chen, D. J., Zdzienicka, M. Z., van Dongen, J. J., and van Gent, D. C. (2009) A DNA-PKcs mutation in a radiosensitive T-B-SCID patient inhibits Artemis activation and nonhomologous end-joining. *J. Clin. Invest.* **119,** 91–98
38. de Miranda, N. F., Björkman, A., and Pan-Hammarström, Q. (2011) DNA repair: the link between primary immunodeficiency and cancer. *Ann. N.Y. Acad. Sci.* **1246,** 50–63
39. Huang, Y., Giblin, W., Kubec, M., Westfield, G., St Charles, J., Chadde, L., Kraftson, S., and Sekiguchi, J. (2009) Impact of a hypomorphic Artemis disease allele on lymphocyte development, DNA end processing, and genome stability. *J. Exp. Med.* **206,** 893–908
40. Jacobs, C., Huang, Y., Masud, T., Lu, W., Westfield, G., Giblin, W., and Sekiguchi, J. M. (2011) A hypomorphic Artemis human disease allele causes aberrant chromosomal rearrangements and tumorigenesis. *Hum. Mol. Genet.* **20,** 806–819
41. Rivera-Munoz, P., Abramowski, V., Jacquot, S., André, P., Charrier, S., Lipson-Ruffert, K., Fischer, A., Galy, A., Cavazzana, M., and de Villartay, J.-P. (2016) Lymphopoiesis in transgenic mice over-expressing Artemis. *Gene Ther.* **23,** 176–186
42. de Miranda, N. F., Peng, R., Georgiou, K., Wu, C., Falk Sörqvist, E., Berglund, M., Chen, L., Gao, Z., Lagerstedt, K., Lisboa, S., Roos, F., van Wezel, T., Teixeira, M. R., Rosenquist, R., Sundström, C., Enblad, G., Nilsson, M., Zeng, Y., Kipling, D., and Pan-Hammarström, Q. (2013) DNA repair genes are selectively mutated in diffuse large B cell lymphomas. *J. Exp. Med.* **210,** 1729–1742